The Design and Fabrication of Three-Chamber Microscale Cell Culture Analog Devices with Integrated Dissolved Oxygen Sensors

Aaron Sin,[†] Katherine C. Chin,[†] Muhammad F. Jamil,[†] Yordan Kostov,[‡] Govind Rao,[‡] and Michael L. Shuler*[,†]

School of Chemical and Biomolecular Engineering, Cornell University, 120 Olin Hall, Ithaca, New York 14850, and Department of Chemical Biochemical Engineering, University of Maryland Baltimore County, Baltimore, Maryland 21250

Whole animal testing is an essential part in evaluating the toxicological and pharmacological profiles of chemicals and pharmaceuticals, but these experiments are expensive and cumbersome. A cell culture analog (CCA) system, when used in conjunction with a physiologically based pharmacokinetic (PBPK) model, provides an in vitro supplement to animal studies and the possibility of a human surrogate for predicting human response in clinical trials. A PBPK model mathematically simulates animal metabolism by modeling the absorption, distribution, metabolism, and elimination kinetics of a chemical in interconnected tissue compartments. A CCA uses mammalian cells cultured in interconnected chambers to physically represent the corresponding PBPK. These compartments are connected by recirculating tissue culture medium that acts as a blood surrogate. The purpose of this article is to describe the design and basic operation of the microscale manifestation of such a system. Microscale CCAs offer the potential for inexpensive, relatively high throughput evaluation of chemicals while minimizing demand for reagents and cells. Using microfabrication technology, a three-chamber ("lung"-"liver"-"other") microscale cell culture analog (μCCA) device was fabricated on a 1 in. (2.54 cm) square silicon chip. With a design flow rate of 1.76 μL/min, this μCCA device achieves approximate physiological liquid-to-cell ratio and hydrodynamic shear stress while replicating the liquid residence time parameters in the PBPK model. A dissolved oxygen sensor based on collision quenching of a fluorescent ruthenium complex by oxygen molecules was integrated into the system, demonstrating the potential to integrate real-time sensors into such devices.

1. Introduction

Toxicological and pharmacological testing are crucial in the chemical and pharmaceutical industries. Potential pharmaceuticals have to be screened for efficacy as well as possible toxicity. In chemical industries, toxicity profiles are important in determining the safe exposure level and first aid mechanisms for household and commercial chemicals. Whole animals are commonly used to determine these toxicological and pharmacological profiles, but these experiments are generally expensive and lengthy to perform. There is also considerable doubt whether results from animal tests can be extended reliably to human beings. Alternatives to animal studies include in vitro cell cultures and computer models.

To help solve this problem, mammalian cell cultures (which include human cells) have been used to obtain mechanistic information for xenobiotic (foreign chemical) metabolism. Researchers have also combined this mechanistic information with physiological information such as blood flow and organ volumes to create physiologically based pharmacokinetic (PBPK) models (*1*, *2*). A PBPK model mathematically simulates the absorption, distribution, metabolism, and elimination (ADME) processes of living systems, providing a method to link mechanistic data obtained in in vitro cell cultures to system-wide toxicological and pharmacological information. However, a realistic PBPK model often requires parameters, particularly those associated with the kinetics of metabolism, that are difficult to estimate. Further, a prime limitation on a PBPK model is that all relevant mechanisms, whether direct or indirect, must be anticipated and included in the model. Often, secondary effects are not explicitly included.

A cell culture analog (CCA) system is a physical replica of the PBPK model (*3*). Mammalian cells are cultured in different compartments to represent organs, which in turn are interconnected by circulating cell culture medium that acts as a blood surrogate. Design parameters such as compartment residence times and flow distibution are based on the corresponding PBPK model. Using representative cell types in the compartments, one can obtain system-wide rate parameters that can then be used to refine the PBPK model. In addition, because mammalian cells from different species of origin can be applied to the CCA, this system provides a potential means of studying cross-species extrapolation of toxicological and pharmacological profiles.

The accuracy of the PBPK parameters obtained from the CCA depends very much on the authenticity of tissue

* To whom correspondence should be addressed. E-mail: mls50@cornell.edu.
[†] Cornell University.
[‡] University of Maryland Baltimore County.

10.1021/bp034077d CCC: $27.50
Published on Web 11/05/2003

constructs. Therefore, it is important that the CCA compartments provide a physiologically realistic environment. Nonphysiological conditions in parameters such as liquid-to-cell ratio and shear stresses could potentially give rise to less than authentic metabolic and physiological functionalities from the cells. Two previous CCA systems have been constructed in our group (*3*−*5*). The first prototype involved milk dilution bottles for the different compartments. Because mammalian cells grew on the bottom of these milk dilution bottles, the liquid-to-cell ratio (>1000:1) (*3*) was far from physiological (1:2). The second system used a packed bed approach, which brought the liquid-to-cell ratio (1:1) closer to physiological levels but did not achieve physiological residence times (*5*) because of constraints on flow in a packed bed of incompressible spheres.

Also, a more realistic environment may be obtained if the characteristic length scale in a physiological system is duplicated. With biological length scales being on the order of 10 μm, microfabrication techniques can be ideal for creating features with similar dimensions (*6*). This advantage has been recognized previously. For example, a microphysiometer is a microfabricated device that detects functional responses from cells by measuring the change of extracellular pH (*7*). This device has been extended to detect receptor-mediated events (*8*) as well as to probe toxicology and pharmacological profiles (*9*, *10*). However, the response of the microphysiometer is still based on a single cell type, which cannot model secondary effects of xenobiotic metabolism addressed by the CCA.

Drawing from the strength of a CCA system in capturing secondary effects and a possibly more physiologically realistic environment in the microscale, we have developed the microscale cell culture analog (μCCA) device. Because of the miniaturization, the μCCA device requires a smaller amount of cells and less test chemical than the macroscopic counterpart. This reduction in material requirement enables the use of scarce authentic cells or tissues constructs, which can in turn help provide a more realistic representation of the organ compartments. Moreover, the smaller device sizes facilitate simultaneous operation of multiple μCCA devices and allow more efficient and reliable experimental designs.

A consequence of miniaturization is that the type of analysis that can be done on the system is limited. Because of the small volume (150 μL or less), it is more difficult to remove samples for analysis without disturbing the dynamics of the system. Integrated real time sensors would provide the ideal means for monitoring key parameters in the μCCA device.

Construction of a dissolved oxygen (DO) sensor was chosen as the proof-of-concept integrated sensor for the μCCA device. Because oxygen is a key substrate in animal cell metabolism (*11*), one concern for the design of the μCCA device is the adequacy of gas exchange during the device operation.

Clark electrodes have been the industry standard for oxygen measurement for more than 3 decades (*12*, *13*). However, because Clark electrodes operate on the principle of oxygen reduction at the electrode, the sensor actually consumes oxygen. Especially for a microfluidic device, this oxygen consumption could disturb the actual DO level in the system. A fluorometric sensor provides a noninvasive alternative, which relies on the quenching a fluorescent ruthenium complex by collision with oxygen molecules (*13*, *14*). This collision event quenches the fluorescence of the ruthenium dye and can be measured through change in intensity and lifetime. Lifetime measurement is preferred to intensity-based sensing, because it is not affected by problems such as photobleaching, probe concentration, and drift in excitation source (*15*).

In this paper, we describe the design and basic operation of a three-chamber ("lung"-"liver"-"other") μCCA device. We also describe the integration of a fluorescence lifetime-based oxygen sensing system based on a system described by Kostov et al. (*16*).

2. Experimental Section

Silicon μCCA Fabrication. A preliminary description of the design of the device is provided in Sin et al. (*17*). The silicon device was fabricated using standard lithography−etching techniques performed in the Cornell Nanofabrication Facility. The desired pattern was designed on CAD (Cadence; Fishkill, NY), converted, exposed, and developed onto a chrome-coated glass mask using electron-bean lithography (Leica/Cambridge EBMF 10.5/CS; Frankfurt, Germany). Two layers of fabrication were required, first a 20 μm deep etch and then a 100 μm deep etch, each with its own mask.

The prototype μCCA devices were fabricated on silicon as opposed to glass because channels with vertical sidewalls can be relatively easily fabricated using reactive ion etching. For the first layer of fabrication, a singled polished (350 μm thick) 3.00 in. (76.2 mm) diameter silicon wafer (Silicon Quest; Santa Clara, CA) was primed with P20 primer (Shipley; Marlborough, MA) to remove any moisture on the surface and spin coated with a ∼1.0 μm thick layer of Shipley 1813 photoresist (Shipley) at 3000 rpm. Pattern was transferred from the mask by exposing the wafer to UV light (405 nm wavelength) for 2.5 s, using a contact aligner (AB-M HTG 3HR Contact-Proximity Aligner; San Jose, CA). The wafer was subsequently developed for 1 min in MF 300 developer solution (Claricut; Somerville, NY). Etching was performed in an inductively coupled plasma reactive ion etcher (Plasmatherm 770; Zurich, Switzerland) at an etching rate of ∼2μm/min, to a depth of 20 μm. The photoresist was dissolved from the wafer in heated Microposit Remover 1165 solution (Shipley) bath at 60 °C for 20 min. Finally, any stubborn resist was stripped using oxygen plasma etching (Branson/IPC P2000 Barrel Etcher; San Jose, CA) at 150 W power for 5 min.

The second layer of fabrication involves the same steps as the first one, except that ∼1.5 μm thick layer of Shipley 1827 photoresist was spun onto the wafer at 3000 rpm, after the priming step. Using the contact aligner, the second layer pattern was aligned to the etched features on the silicon wafer, and the photoresist was exposed to 405 nm UV light for 10 s. After development, the wafer was etched in the Plasmatherm 770 again, but to a depth of 100 μm, which took about 50 min. Finally, the photoresist was dissolved away in the heated resist bath and then etched by oxygen plasma using the same settings as the first layer.

At this point, the silicon wafer consists of four μCCA devices. The individual μCCA devices were scored by an infrared laser (MEL 40 laser system, Florod Corporation; Gardena, CA). The 1065 nm laser was focused on the wafers, set at 5000 Hz modulation and 50 mJ energy (28A current), while the wafer was moved by a computer controlled stage at ∼0.2 mm/s. The scored wafer was separated by gentle tapping.

μCCA Device Assembly. A 1.5 in. × 2.5 in. (3.8 cm × 6.4 cm) Plexiglas (poly(methylmetacrylate); PMMA) housing was fabricated to enclose the open channels on the silicon μCCA device. The top and bottom pieces were machined from a nominal 1/8 in. (3.2 mm) and 1/4 in.

(6.4 mm) thick Plexiglas sheet (McMaster-Carr; New Brunswick, NJ), respectively. The top piece consisted of counterbored holes for the inlet and the outlet of the device, with diameters of 740 μm (drill size no. 69; Small Parts; Miami Lakes, FL) at the top half of the channel and 610 μm (drill size no. 73; Small Parts) at the bottom. The bottom piece consisted of a 1.01 in. square (2.56 cm) recess for the silicon chip of 2 mm depth. Silicone sheets (0.5 mm thick Press-to-seal silicone; Grace Bio-Labs; Bend, OR) cut to 1.0 in. (2.5 cm) square sizes were used to adjust the depth of the well such that the silicon chip sat flush (determined by touch) with the PMMA surface. The completed casing was assembled using stainless steel 4−40 screws (Small Parts).

To assemble the μCCA device, the silicon chip was placed into the recess in the Plexiglas bottom. A drop (~0.2 mL) of liquid (cell culture medium or water) was placed on top of the silicon chip, removing any air bubbles present on the chip surface. The Plexiglas top was placed on, pushing the drop of liquid off the sides and through the inlet and outlet holes. Care should be taken by placing this top in a tilted manner such that no air bubbles are trapped in the channels. The recirculation loop is completed by a peristaltic pump (205S; Watson-Marlow; Wilmington, MA) running at 0.75 rpm to give 2 μL/min flow rate, in conjunction with 0.25 mm inside diameter Pharmed tubings (Cole-Parmer; Vernon Hills, IL). The connections between the tubings and the μCCA was facilitated by the 1 cm tip section of a gel-loading tip (VWR International; New Brunswick, NJ), which fits snugly into the counterbored holes in the Plexiglas top without using any glue. A 100-μL fluid reservoir, used as a debubbler, was constructed from a well from a 8-well strip plate (Corning Costar; VWR), sealed with a Teflon-lined silicone cover (996050MR-96; BioTech Solutions, Mt. Laurel, NJ). A 2-cm section of a 24-gauge stainless steel needle (Small Parts) was used to interface between the reservoir and the Pharmed tubing.

Residence Time Measurement. After the μCCA device was assembled, deionized (DI) water was pumped through the device. After making sure that no fluid leaked within 10 min, the liquid source was switched to silicon oil (Sigma-Aldrich; St. Louis, MO). The advancement of the water−oil interface through the chambers was observed under a metallurgical (reflective) microscope (Fisher Scientific; Pittsburgh, PA) and timed with a stopwatch. This experiment was repeated at least three times for each chamber.

***μ*CCA Experiments.** The silicon μCCA devices were immersed in heated piranha solution (30:70 hydrogen peroxide/sulfuric acid, 90 °C) for 2 h to remove any organic residues. They were subsequently rinsed with deionized (DI) water and dried off with compressed air. Care should be taken not to have inorganic salt solution (including tap water) dry on the silicon surface. Poly-D-lysine (Sigma-Aldrich) was dissolved in DI water at 0.1 mg/mL concentration, 5- and 10-μL drops of which were manually placed using a micropipet onto the lung and liver chambers, respectively. The chips were left to dry on a 60 °C hot plate for about 15 min, then immersed in 70% ethanol, and flamed dry in the tissue culture hood. This polylysine coating step was performed to improve the hydrophilicity of silicon and facilitate the immobilization of more specific extracellular matrix proteins. The lung and liver chambers were then coated with 5 μL of human plasma fibronectin solution (50 μg/mL in DI water; Chemicon International; Temecula, CA) and 10 μL of rat tail type I collagen solution (50 μg/mL in 0.02 N acetic acid/DI water; Collaborative Biomedical Products; Bedford, MA), respectively, under sterile conditions. The silicon chips were subsequently placed in the 37 °C incubator for 2 h for the protein to attach. Finally, the excess protein solution was rinsed off with sterile filtered DI water, and the chips were left to dry overnight on a 37 °C hot plate.

L2 and H4IIE cell lines were obtained from ATCC (Manassas, VA) and maintained with DMEM/F12 (1:1) tissue culture medium (Life Technologies; Rockville, MD) supplemented with 10% fetal bovine serum (FBS). The addition of FBS provides the growth factor necessary to promote cell proliferation. To plate cells onto the silicon chip, cells in tissue culture flasks were trypsinized and resuspended in FBS-supplemented medium to final concentrations of $\sim 1.3 \times 10^6$ cells/mL for L2 and $\sim 2.5 \times 10^6$ cells/mL for H4IIE. The number of cells from each flasks was estimated using a hemocytometer, and the cell suspension was centrifuged down (1000 rpm, 5 min) and resuspended to achieve the final cell concentrations. The protein-coated chips were placed individually into 60-mm Petri dishes (Corning brand; VWR), on top of two pieces of 45-mm diameter filter paper (Whatman no. 3; VWR). The filter paper in each Petri dish was soaked with 1 mL of FBS-supplemented medium to maintain humidity inside the dish. Drops of cell suspension (5 μL for L2 and 10 μL for H4IIE) were manually placed onto the lung and liver chambers using a micropipet. The chips were then placed in the 37 °C incubator for the cells to attach. After 4 h, 5 mL of FBS-supplemented medium was added to each Petri dish to maintain the cells overnight.

μCCA experiments were performed the day after cell plating. The μCCA devices were assembled as described above. DMEM/F12 (1:1) tissue culture medium supplemented with 0.5% bovine serum albumin (BSA) and 0.1% dimethyl sulfoxide (DMSO) was used as blood surrogate. BSA was used instead of FBS such that the tissue culture medium for the toxicity experiments remains chemically defined. Also, cell proliferation was not promoted during the 1−6 h toxicity experiments, as no growth factors (from FBS) were present in the medium.

The assembled μCCA devices were examined under the metallurgical microscope and images of cultured cells in the lung and liver chambers were recorded on VHS tapes using a color NTSC CCD camera (Fisher Scientific). The peristaltic pump and the μCCA devices were moved to a 37 °C incubator, where the BSA supplemented medium was recirculated for 1−6 h, depending on the experiment. At the end of the experiment, the cells were stained with trypan blue exclusion dye by switching the fluid reservoirs to one containing a 50:50 mixture of BSA-supplemented medium and 0.4% trypan blue (Sigma Aldrich). The peristaltic pump was kept running for another 20 min to ensure that the trypan blue solution had flowed through the μCCA chip. After photographs of the L2 and H4IIE cells in the lung and liver chambers were recorded again and compared against the before photographs. Images from the VHS recording were converted to digital images using an image capture card (DT3120, Data Translation, Marlboro, MA).

After each experiment, the μCCA chips were removed from the Plexiglas casing, immersed in 70% ethanol, and then sonicated for 15 min to remove all cell debris. It was important that the chips be immersed in liquid at all times to prevent inorganic salt buildup on the silicon surface. These chips were then cleaned in a heated piranha bath and reused.

Oxygen Sensing. A 3.0 mm × 3.0 mm × 0.15 mm recess was machined into the bottom of the chip house cover for integration of the oxygen sensor patch. The

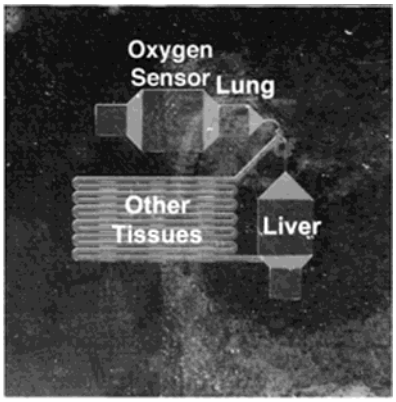

Figure 1. Photograph of the fabricated 1 in. square silicon μCCA device. The "other tissues" compartment and the connecting channels between compartments are etched 100 μm deep, and the rest of the features are etched 20 μm deep.

oxygen sensor patch would then be interfacing with the μCCA medium on one side while attached to the Plexiglas on the other side. The sensing was performed at the oxygen sensor chamber (see Figure 1).

The tris(4,7-diphenyl-1,10-phenanthrolin)rutheniumm-(II) dichloride complex ($Ru(dpp)_3Cl_2$) was synthesized at the Center for Fluorescence Spectroscopy, University of Maryland, Baltimore. This ruthenium complex or dye was immobilized onto a resin (LiChroSorb 100; Merck; Darmstadt, Germany) at about 1:10 dye:resin ratio by weight. The immobilization was done by dissolving the ruthenium dye in 33% methanol in water, and resin was added to the solution until the color of the solution turns pale. The dye-containing resin particles were then filtered out of the solution and rinsed with chloroform.

The dye particles were further encapsulated in a silicone (poly(dimethylsiloxane), PDMS) matrix to form the oxygen sensor patches. Sylgard 184 (Dow Corning; Midland, MI) silicone was used in this study, which consisted of two parts: an elastomer gel and a platinum-based curing agent. On a microscope slide, 1 part curing agent, 10 parts elastomer gel, and 1 part dye particles by weight were added in that order before mixing with a spatula. The order of ingredient addition was important in ensuring the homogeneity of the resultant oxygen patch. This mixture was left to cure on the microscope slide for 2 h in the fume hood, which helps prevent the deposition of large dust particles. The partially cured silicone prepolymer was added into the recess in the Plexiglas top, which were then cured in a 60° oven for 3−7 days. The cured oxygen sensor patches were stabilized at room temperature for at least 24 h before use.

A blue silicon LED (LNG992CFBW; Panasonic; Secaucus, NJ) was used as the excitation source, with its emission filtered with a 460 ± 15 nm filter. The fluorescent emission from the oxygen sensor patch was performed by a photodiode module (S1223-01, Hamamatsu; Bridgewater, NJ) with a mounted 590 ± 20 nm bandpass interference filter. The photodiode response was amplified through a simple circuit and the phase measurements were then made using a lock-in amplifier (EG&G 5110; Princeton, NJ). This lock-in ampifier was also used to supply the 75-kHz square wave LED modulation. The amplifying circuit was powered by a ±5 V unregulated DC power supply, taken from an old ATX form-factor computer case. Finally, the phase measurement output was recorded using a voltage data logger (IQ-VmA-40; Measurement Computing; Middleboro, MA).

For the response time measurements, the μCCA device was assembled as described above. Pure nitrogen (compressed nitrogen tank; Airgas Mid-Atlantic; Radnor, PA) and air (generated by a pressure/vacuum pump; Welch 2545, Thomas Industries; Skokie, IL) were injected into the μCCA device alternately at 15 psi pressure. Three sets of each experiments (with different sensor patches) were performed. To measure the DO level during a μCCA experiment, the entire μCCA and oxygen sensing setup, including the lock-in analyzer, were moved into a 37 °C, 5% CO_2 incubator for the duration of the experiment. This experiment was performed in duplicate.

Table 1. Chamber Dimensions and Residence Times (τ) of the Microscale CCA Device

	width	length	depth	design (*21*)	actual τ
lung	2.0 mm	2.0 mm	20 μm	2.5 s	2.5 ± 0.7 s
liver	3.2 mm	4.0 mm	20 μm	30 s	32 ± 14 s
other tissues	340 μm	110 mm	100 μm	204 s	179 ± 21 s

3. Results and Discussions

***μ*CCA Device Design.** Although a PBPK or CCA may be designed, in principle, with as many compartments as there are tissues in the body, it is customary to lump related tissues into a single compartment. A very simple system is lung-liver-other tissues. For the initial proof-of-concept experiments for the CCA, this system was chosen to study naphthalene metabolism (*3*, *5*). Lung tissues are sensitive to naphthalene metabolites in some animals (e.g., mice), and the liver was chosen in the model CCA system to represent tissues capable of metabolizing naphthalene and naphthalene metabolites with P450 monooxygenases.

To facilitate comparison with previous results, a three-chamber μCCA (lung-liver-other tissues) was designed and constructed. The prototype was designed on the basis of the following constraints:

1. The ratio of the chamber sizes and the liquid residence times in each compartment should be physiologically realistic.
2. Each chamber should have a minimum of 10^4 cells to facilitate analysis of chemicals.
3. The hydrodynamic shear stress on the cells should be within physiological values (<2 dyn/cm^2) (*18*).
4. The liquid-to-cell ratio should be close to the physiological value (1:2) (*19*).

A fabricated μCCA device is shown in Figure 1. The lung and liver chambers replicate the corresponding compartments in the PBPK model and contain the representative cell culture; the other tissues chamber mimics the liquid holdup of the test chemical in nonreactive and nonabsorptive tissues and consists of no cells. The μCCA design consists of two different feature depths: the lung and liver chambers, along with their fluid diffusers, are 20 μm deep, and the connecting channels and the other tissues chamber are 100 μm deep. Table 1 shows the μCCA chamber dimensions and residence times. The error values in the actual residence times represent the standard deviations among three measurements.

In this design, fluid first flows through the lung chamber, after which 25% of the fluid enters the liver chamber and 75% goes into the other tissues chamber. The fluid from both liver and other tissue chambers is subsequently combined, taken out of the chip by an external pump, and then recirculated back to the inlet. The liver chamber and other tissue chamber were designed such that the hydrodynamic resistance (pressure drop) through each chamber was the same. With the matched pressure drops, the fluid flow split could be achieved passively by designing the channel cross-sec-

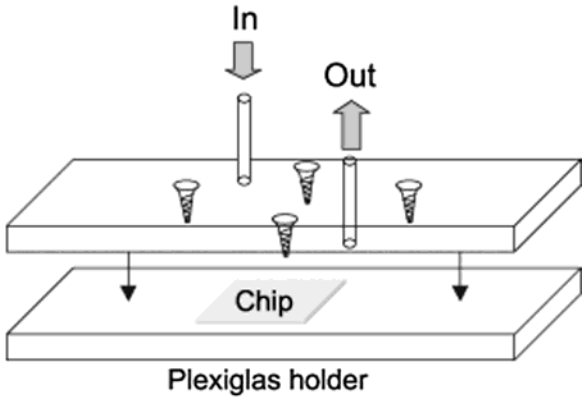

Figure 2. Schematic of the Plexiglas chip house for the μCCA device.

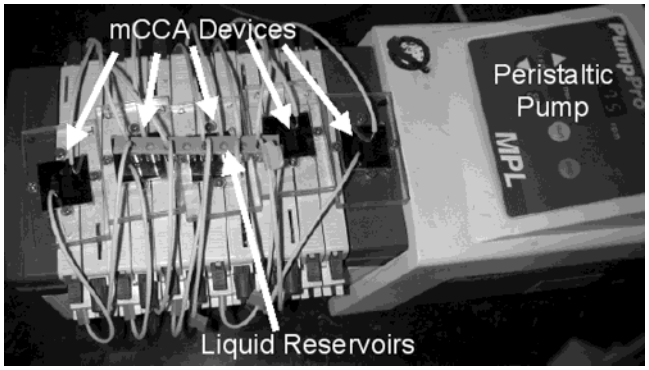

Figure 3. Photograph showing of the complete μCCA experimental setup.

tions according to the flow split ratio. Before and after each cell culture chamber, the fluid channels were gradually expanded or contracted at 45° angles by diffuser structures. These diffusers consist of 20 μm square pillars at 20 μm height set up at a void fraction of 3/4, which help prevent the fluid from streaming through the middle of the chambers. The pillars also help trap air pockets and detached cells from entering the next chamber. An extra 4 mm square chamber etched 20 μm in depth (10-s residence time) was inserted in front of the lung chamber to allow time for the fluid flow from the external pump to stabilize.

The hydrodynamic shear stresses are 6.7 and 0.8 dyn/cm^2 for lung and liver chambers, respectively. Note that the lung chamber shear stress is higher than the physiologically limit of 2 dyn/cm^2 (*18*) expected for body tissue although less than the hydrodynamic shear stress range experienced by endothelial cells that line blood vessels (8−14 dyn/cm^2). The liquid-to-cell ratios are about 4:1 for the lung chamber and 2:1 for the liver chamber, calculated using the cell volume numbers estimated by Ghanem (*19*).

Figure 1 shows a photograph of the fabricated silicon μCCA chip. Since the chip consists of open channels, a Plexiglas chip house was also designed to enclose the channels (see Figure 2). To achieve both liquid residence times and physiological hydrodynamic shear rate, the flowrate was calculated to be 1.76 μL/min. This gives rise to Reynold's numbers in the order of 0.1. The complete experimental setup is shown in Figure 3.

***μ*CCA Device Testing.** To verify that the microfluidic features in the μCCA device were fabricated according to the design parameters, residence times in each of the chambers were measured. Since delicate control of the flow rate was not available with the macroscopic peristaltic pump, 2 μL/min flow rate was used instead. As shown in Table 1, the actual residence times compares fairly well with design values despite the slightly higher flowrate used. This demonstrated that the passive flow split after the lung chamber gave the fluid distribution desired and that fluid flow in microfluidic channels can be estimated to the first order by the Hagen−Poiseuille equation in classical fluid mechanics.

The operation of the μCCA device with recirculation for 6−24 h (at a rate of ~10 cycles per hour) is significantly more difficult than one-pass flow-through for residence time measurements. As shown in Figure 3, there is a 100-μL reservoir for each μCCA device. Experiments were initially performed without the reservoir, but it was found that air pockets tended to accumulate in the system, causing leakage. This introduction of air could be due to a mismatch between the push−pull cycles of the peristaltic pump, causing air bubbles to be sucked into the system through the gaps between gel loading tips and the inlet hole. The reservoir isolates the pull and push actions by separating them into two tubings and also provide a debubbler should air bubbles enter the system. The volume of 100 μL was necessary to keep a high enough liquid height such that the end of the stainless steel needles were always immersed.

With residence times of the individual chambers near physiological values, the existence of a 100-μL reservoir (50-min residence time) would sacrifice the physiological realism. We have also designed an integratable micropump (*20*) that should alleviate the need for such a reservoir. The effect of the reservoir on ADME and toxicity can be addressed in the corresponding PBPK model.

After verifying the fluid flow characteristics in this μCCA device, the ability of this device to maintain cell viability was experimentally determined. Early experiments indicated that L2 and H4IIE cell viability could be maintained for at least 24 h (*17*). L2 and H4IIE cells were chosen in previous CCA systems to represent lung and liver tissues, respectively (*3*, *5*). These experiments were performed using poly-D-lysine-coated silicon μCCA devices without piranha cleaning between each experiments. Organic residues such as proteins secreted by the cells and adsorbed naphthalene and metabolites can potentially accumulate among experiments.

Removal of organic residues from the silicon surface using piranha solution was introduced to prevent contamination of surface-adsorbed test chemical between experiments. Fresh poly-D-lysine coating was applied before each experiment, and L2 and H4IIE cells cultured on the μCCA devices showed morphologies comparable to the respective cells cultured in tissue culture flasks. However, when fluid flow was introduced, the cells were observed to "ball up" after about 1 h and started to lift off from the silicon surface after about 4 h. This phenomenon was observed even at 0.5 dyn/cm^2 of shear stress and was more obvious in L2 cells, since L2 cells are naturally more elongated than the cuboidal H4IIE cells. It was hypothesized that proteins in the medium could aid in cell attachment, but 6-h experiments recirculated with FBS-supplemented medium and BSA-supplemented medium brought about no observable difference in the L2 and H4IIE attachment in the μCCA device.

Further experimentation demonstrated that the fibronectin coating helped alleviate the "lifting off" problem for L2 cells, for shear stresses ranging from 0.5 to 6.7 dyn/cm^2. Collagen coating improved the attachment of H4IIE cells in a similar fashion. Once again, the L2 and H4IIE cell population remained fully viable after at least

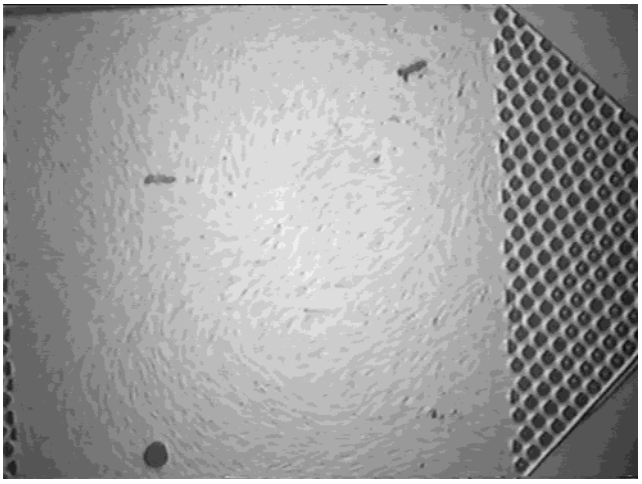

Figure 4. Picture of the ideal growth pattern of L2 in the lung chamber: note the quasicircular pattern of cell growth and the alignment of cells along each other. The diffusers were also shown to the entrance and exit of this lung chambers. The dark spots inside the chamber were defects in silicon etching. This photograph was taken with a 4× objective with a CCD camera with a ~15× lens.

6 h of μCCA operation as confirmed by trypan blue exclusion dyes.

Cell plating density also played a role in the shear sensitivity of these cells. When the ideal plating density was reached, the cell morphology was maintained exactly after at least 6 h of fluid flow. Cell culture that was more sparse or more dense than this ideal plating density "balled up" after 4 h of fluid flow but did not lift from the surface. It was observed that the ideal plating density gives rise to a very specific cell growth pattern that is quasicircular with the cells aligning along each other (see Figure 4). This ideal cell growth pattern was difficult to obtain in these initial experiments. This fluctuation in cell plating density was due to the lack of precision with hemacytometer counting ($\pm 10^4$ cells/mL) combined with the small number of cells required (~7000 cells for the lung chamber and ~25 000 cells for the liver chamber). Consequently more devices than needed were seeded (e.g., 20) and 4−6 devices with cell confluency and morphology closest to that shown in Figure 4 were chosen for experiments.

Oxygen Sensing. The working principle of the oxygen sensor design is shown in Figure 5. The sensor patch was integrated into the top piece of the Plexiglas chip house, interfacing with the recirculating medium. Dissolved oxygen diffuses through the silicone matrix, collides with the ruthenium complex at the top of the sensor patch, and causes change in the fluorescence lifetime, which is the measured output. The theory behind fluorescence lifetime detection of oxygen has been described previously (*13*, *15*, *16*).

Through the Plexiglas, the modulated blue LED excites the sensor patch at a 45° angle and the photodiode detects the fluorescence emission orthogonal to the plane of fluid flow. The LED and photodiode assembly are shown in Figure 6. A photograph of the complete setup, including the μCCA device, peristaltic pump, and the lock-in amplifier, is shown in Figure 7.

Because oxygen has to diffuse through the silicone matrix, the thickness of the oxygen sensor patch is important to the response time. The law of diffusion would indicate that the sensor patch be produced as thin as possible. However, a thin sensor patch would encapsulate less dye particles, leading to a lower fluorescence

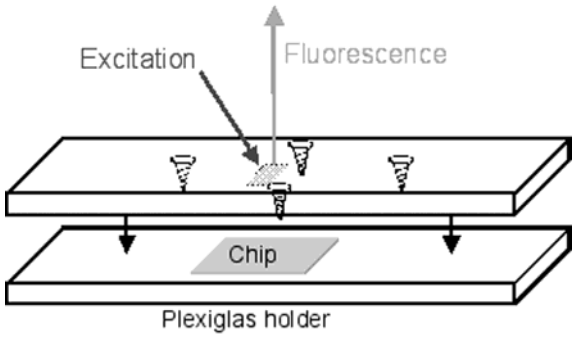

Figure 5. Schematic showing the working principle of oxygen sensor integrated in the μCCA device.

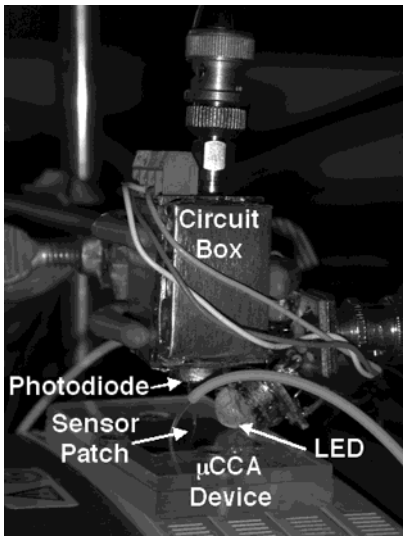

Figure 6. Photograph showing the excitation and detection circuit box and the μCCA device with integrated oxygen sensor.

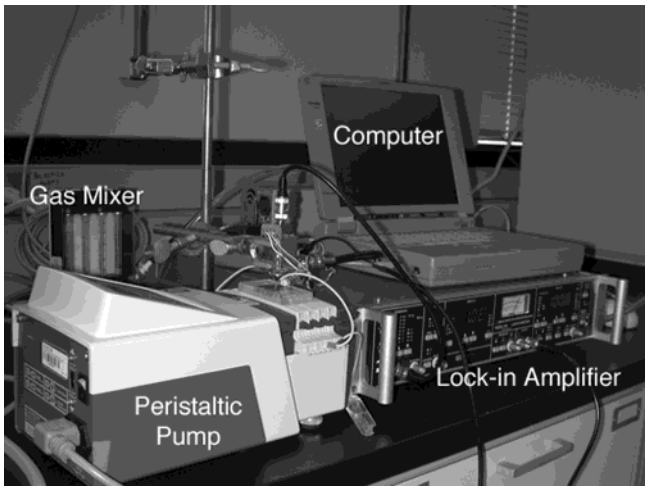

Figure 7. Photograph showing the overall setup of the μCCA oxygen detection.

signal and thus a lower signal-to-noise ratio. Furthermore, a thin sensor patch would involve a shallow recess in the Plexiglas surface, which is difficult to fabricate consistently with traditional machining. It would also be difficult to fill this shallow recess with just the right amount of prepolymer such that the resultant sensor patch would be flush with the Plexiglas surface and maintain a good seal on the μCCA device. After numerous trials, the final thickness was determined to be 150 μm, which is equivalent to the thickness of about 1.5 sheets of regular 20 pound paper. This sensor gave a response

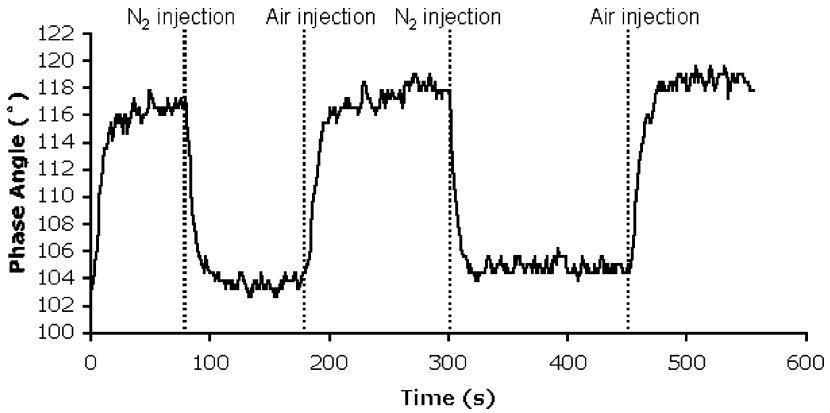

Figure 8. Actual response of an integrated oxygen sensor, when input is alternate between gaseous nitrogen and air. Note that the initial phase angle is arbitrary.

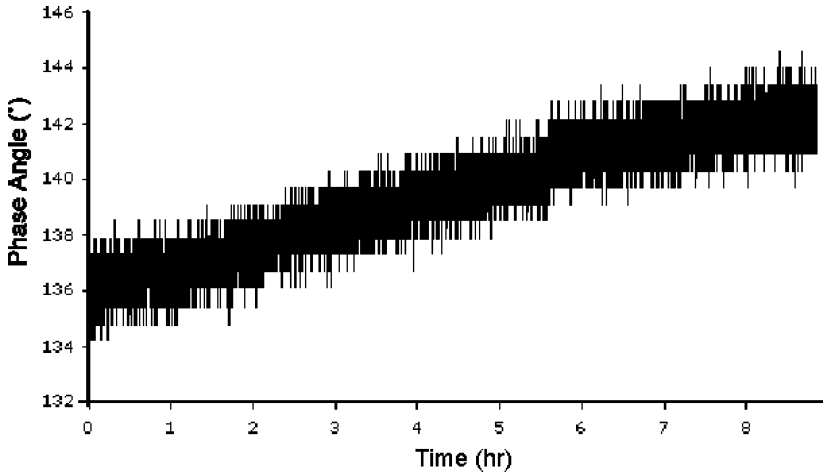

Figure 9. Oxygen sensor reading from a μCCA experiment, with the initial DO level in BSA supplemented medium being 100% (saturated in air). Note that the initial phase angle is arbitrary.

time (defined as the time to reach 90% of the final readout level) of less than 20 s in measuring oxygen levels when air and nitrogen gas were injected alternately (see Figure 8).

Note that the sensors measure the concentration of oxygen in the silicone matrix in equilibrium with the fluid environment. Therefore, the calibration curve of these DO sensors in a gaseous environment was found to be identical to that in an aqueous environment (*13*).

The difference in phase angle between 100% DO (air) and 0% DO was ~14°, which was constant among different sensor patches, given the ±1° resolution limit on the lock-in amplifier (see Figure 8). Note also that the initial phase angle is arbitrary among experiments, but the range in phase angle remains the same. However, as seen in Figure 8, there was some drift in the phase angle measurement by the lock-in amplifier. Some of this drift was eliminated by stabilizing the sensor patch in room temperature for 24 h, after ensuring that the silicone has completely cured in the 60° oven. However, a drift of ~0.7°/h still remained after the stabilization treatment. Further experimentation demonstrated that this 0.7°/h drift was due to the electronic equipment, as the phase angle would return to the initial number if the lock-in amplifier and the power supply were reset (switched off and then switched back on after about a minute).

The oxygen sensor was also tested directly in a μCCA device with cultured L2 and H4IIE cells. Two experiments were performed where the DO in the μCCA device was monitored for at least 6 h periods without the presence of xenobiotic chemical, which resulted in virtually identical DO measurements. The BSA-supplemented medium was equilibrated with air at the beginning of the experiment (DO = 100%). As seen in Figure 9, apart from the ~0.7°/h drift in the phase angle, the DO of the device remained constant over the period of experiment.

The lack of response in the aqueous environment was likely due to the diffusion of oxygen through the tubing walls. According to product literature, the oxygen permeability of Pharmed tubings is $P_M = 9.08 \times 10^{-10}$ (mmol O_2·mm)/(s·cm^2·cmHg) at room temperature, which gives rise to a k_La of 2.4×10^{-3} mmol O_2 s^{-1} cm^{-3}. Solving eq 1 using parameters listed in Table 2, deoxygenated solution (0% DO) in the reservoir becomes 76% oxygenated when it reaches the μCCA device. Additional oxygen diffusion could occur at connections between the gel-loading tips or the stainless steel needles. This estimation, along with the experimental results (see Figure 9) indicate that the μCCA device has adequate oxygen exchange with the environment.

$$\frac{\partial \mathrm{DO}}{\partial t} = k_L a(100\% - \mathrm{DO})$$

$$k_L a = \left(\frac{P_M}{x_T}\right)\left(\frac{A}{V}\right)\left(\frac{p^*}{c^*}\right) \quad (1)$$

Conclusion

We have described a μCCA device useful for studying toxicology and pharmacological profiles of xenobiotic

Table 2. List of Parameters for μCCA Dissolved Oxygen Calculation

parameter	value	units	explanation
P_M	9.08×10^{-1}	mmol·mm/s·cm²·cmHg	oxygen permeability of Pharmed tubing
x_T	2.0	mm	thickness of the tubing wall
A/V	160	cm^{-1}	surface area-to-volume ratio for liquid in the tubing
p^*	16	cmHg	partial pressure of oxygen in the outside environment
c^*	4.9×10^{-4}	mmol cm^{-3}	saturation concentration of oxygen in aqueous solution
τ_{tubing}	10	min	liquid residence time in the Pharmed tubing

chemicals. This device was fabricated from silicon substrate, complete with a Plexiglas chip house to enclose the channels. Fluid flow characteristics was verified and mammalian cell culture (L2 and H4IIE cells) viability was maintained for at least 24 h.

One concern for the μCCA operation is the adequacy of gas exchange in the system. A noninvasive, fluorescent lifetime-based oxygen sensor has been successfully integrated into the μCCA device. With a sensor patch thickness of 150 μm, response time of less than 20 s was observed in gaseous environment. Experiments also showed that the μCCA prototype has adequate oxygen exchange with the incubator atmosphere in the current configuration.

Because of the smaller size of the μCCA device, multiple experiments can be performed in parallel, which helps reduce random variations when comparing among control and toxicity experiments. Parallel experiments were not possible in previous CCA systems, where the same set of experiments performed on the μCCA device in one sitting would have to be carried out over several days. Additionally, the μCCA device provides more physiologically realistic tissue culture chambers. These improvements give rise to potentially more accurate and physiologically relevant toxicity results when compared to the previous CCA generations. By integrating the oxygen sensor onto the μCCA device, we have also demonstrated the feasibility of integrating sensors in the μCCA device. The appropriate sensors can then facilitate online monitoring of the status of individual cell cultures in the μCCA, which provides significant advantages over traditional cell culture techniques that are generally endpoint studies.

Acknowledgment

Work at Cornell was supported by the Nanobiotechnology Center (NBTC), a STC Program of the National Science Foundation under agreement ECS-9876771, the Cornell Center for Advanced Technology (Biotechnology) with support from New York State Science and Technology Foundation and a consortium of industries, as well as a matching gift from DuPont. Work at UMBC was sponsored by NSF grant BES0091705 and unrestricted funding from DuPont, Fluorometrix, Genentech, Merck, and Pfizer. This work was performed in part at the Cornell Nanofabrication Facility (a member of the National Nanofabrication Users Network) ,which is supported by the National Science Foundation under grant ECS-9731293, its users, Cornell University, and Industrial Affiliates. We would also like to thank Paula Miller, Glenn Swan, and Greg Baxter for their technical assistance.

References and Notes

(1) Gerlowski, L.; Jain, R. Physiological based pharmacokinetic modeling: principles and applications. *J. Pharm. Sci.* **1983**, *72*, 1103−1127.

(2) Quick, D.; Shuler, M. Use of in vitro data for construction of a physiologically based pharmacokinetic model for naphthalene in rats and mice to probe species differences. *Biotechnol. Prog.* **1999**, *14*, 540−555.

(3) Sweeney, L.; Shuler, M.; Babish, J.; Ghanem, A. A cell culture analog of rodent physiology: Application to naphthalene toxicity. *Toxicol. In Vitro* **1995**, *9* (3), 307−316.

(4) Ghanem, A.; Shuler, M. Combining cell culture analogue reactor designs and PBPK models to probe mechanisms of naphthalene toxicity. *Biotechnol. Prog.* **2000**, *16*, 334−345.

(5) Ghanem, A.; Shuler, M. Characterization of a perfusion reactor utilizing mammalian cells on microcarrier beads. *Biotechnol. Prog.* **2000**, *16*, 471−479.

(6) Voldman, J.; Gray, M.; Schmidt, M. Microfabrication in biology and medicine. *Ann. Rev. Biomed. Eng.* **1999**, *1*, 401−425.

(7) McConnell, H.; Owicki, J.; Parce, J.; Miller, D.; Baxter, G.; Wada, H.; Pitchford, S. The cytometer microphysiometer: Biological applications of silicon technology. *Science* **1992**, *257*, 1906−1912.

(8) Hafner, F. Cytosensor microphysiometer: Technology and recent applications. *Biosens. Bioelectron.* **2000**, *15*, 149−158.

(9) Cooke, D.; O'Kennedy, R. Comparison of the tetrazolium salt assay for succinate dehydrogenase with the cytosensor microphysiometer in the assessment of compound toxicities. *Anal. Biochem.* **1999**, *274*, 188−194.

(10) Fischer, H.; Seelig, A.; Beier, N.; Raddatz, P.; Seelig, J. New drugs for the Na^+/H^+ exchanger. Influence of Na^+ concentration and determination of inhibition constants with a microphysiometer. *J. Membr. Biol.* **1999**, *168*, 39−45.

(11) Tilles, A.; Baskaran, H.; Roy, P.; Yarmush, M.; Toner, M. Effects of oxygenation and flow on the viability and function of rat hepatocytes cocultured in a microchannel flat-plate bioreactor. *Biotechnol. Bioeng.* **2001**, *73*, 379−389.

(12) Clark, L. Monitor and control of blood and tissue oxygen tension. *Trans. Am. Soc. Artif. Int. Org.* **1956**, *2*, 41.

(13) Bambot, S.; Holavanahali, R.; Lakowicz, J.; Carter, G.; Rao, G. Phase fluorometric sterilizable optical oxygen sensor. *Biotechnol. Bioeng.* **1994**, *43*, 1139−1145.

(14) Randers-Eichhorn, L.; Bartlett, R.; Frey, D.; Rao, G. Noninvasive oxygen measurement and mass transfer considerations in tissue culture flasks. *Biotechnol. Bioeng.* **1996**, *51*, 466−478.

(15) Lakowicz, J. *Principles of Fluorescence Spectroscopy*, 2nd ed.; Plenum: New York, 1999.

(16) Kostov, Y.; Harms, P.; Randers-Eichhorn, L.; Rao, G. Low-cost microbioreactor for high-throughput bioprocessing. *Biotechnol. Bioeng.* **2001**, *72*, 346−352.

(17) Sin, A.; Baxter, G.; Shuler, M. Animal on a chip: a microscale cell culture analog device for evaluating toxicological and pharmacological profiles. In *Proceedings of SPIE−Microfluidics and BioMEMS*; SPIE: Bellingham, WA, 2001; Vol. 4560, pp 98−101.

(18) Powers, M.; Domansky, K.; Kaazempur-Mofrad, M.; Artemis, K.; Capitano, A.; Upadhyaya, A.; Kurzawski, P.; Wack, K.; Stolz, D.; Roger, K.; Griffith, L. A microfabricated array bioreactor for perfused 3d liver culture. *Biotechnol. Bioeng.* **2002**, *78*, 257−269.

(19) Ghanem, A. Application of a Novel Packed Bed Cell Culture Analog Bioreactor and a Corresponding Pharmacokinetic Model to Naphthalene Toxicology. Ph.D. Thesis, Cornell University, 1998.

(20) Sin, A. Development of a Three-Chamber Microscale Cell Culture Analogue Device. Ph.D. Thesis, Cornell University, 2002.

(21) Gearhart, J.; Jepson, G. H. C., III; Andersen, M.; Conolly, R. Physiologically based pharmacokinetic model for the inhibition of acetylcholinesterase by diisoproplylfluorophosphate. *Toxicol. Appl. Pharmacol.* **1990**, *106*, 295−310.

Accepted for publication September 26, 2003.

BP034077D